

Anticancer Effectivity of Nanocrystals Derived from Mangosteen (*Garcinia mangostana*) Peel Extract on Leukemia HL-60 Cells

Marisca Evalina Gondokesumo¹, Arina Novilla², Sijani Prahastuti³, Hanna Sari Widya Kusuma⁴, Wahyu Widowati^{3*}, Fadhilah Haifa Zahiroh⁴, Dhanar Septyawan Hadiprasetyo^{4,5}, Wahyu Surakusumah⁶

¹Faculty of Pharmacy, Universitas Surabaya, Surabaya, 60293, Indonesia

²Medical Laboratory Science Program, Universitas Jenderal Achmad Yani, Cimahi, 40531, Indonesia

³Faculty of Medicine, Maranatha Christian University, Bandung, 40164, Indonesia

⁴Biomolecular and Biomedical Research Center, Aretha Medika Utama, Bandung, 40163, Indonesia

⁵Faculty of Pharmacy, Universitas Jenderal Achmad Yani, Cimahi, 40531, Indonesia

⁶Biology Study Program, Faculty of Mathematics and Science Education, Universitas Pendidikan Indonesia, Bandung, 40154, Indonesia

*Corresponding author: wahyu_w6@yahoo.com; wahyu.widowati@maranatha.edu

Abstract

Leukemia, characterized by abnormal leukocyte proliferation, ranks ninth in Indonesia as the most common cancer. While treatments such as chemotherapy and radiation effectively target cancer cells, they also pose a risk of damaging healthy blood cells. This has spurred interest in exploring low-toxicity herbal compounds as potential therapies, with mangosteen peel emerging as a widely researched option. Nanotechnology, which has the potential to enhance the bioavailability of herbal compounds, is also a focus of extensive research. This study objective was to assess the impact of Mangosteen Peel Nanocrystal (MPN) on HL-60 leukemia cells by analyzing various parameters, including cytotoxicity, reactive oxygen species (ROS) levels, senescence, and gene expression changes. MPN was prepared with high-speed milling and characterized using particle size analyzers, microscopy, and stability assessments. HL-60 cells were cultured and subjected to MPN treatment. Cytotoxicity was evaluated using WST-8 assays, ROS levels were assessed using flow cytometry, and senescence analyses using Senescence-Associated β -Galactosidase Staining. AKT and FLT-1 gene expression were determined via qRT-PCR. MPN has been successfully characterized as a nanoparticle based on size, stability, and morphology. MPN has an impact on leukemia cells by increasing cytotoxicity, decreasing ROS levels, inducing senescence, and modulating AKT and FLT-1 gene expressions. The findings suggest potential implications for MPN in targeting leukemia cells. The study sheds light on the promising effects of MPN in leukemia cell models, indicating its potential applications in targeting cancer cells, inducing senescence, decreasing ROS levels, and modulating gene expressions related to cell survival and proliferation.

Keywords

Anticancer, *Garcinia mangostana*, HL-60 Cells, Leukemia, Nanocrystal

Received: 30 April 2024, Accepted: 11 December 2024

<https://doi.org/10.26554/sti.2025.10.1.228-237>

1. INTRODUCTION

Leukemias are malignant disorders characterized by leukocytes abnormal proliferation in the bone marrow or blood (Dong et al., 2020). According to data from the Global Cancer Observatory (2020), Indonesia reported a leukemia incidence rate of 5.9 to 7.3 cases per 100,000 individuals, making it as the country's ninth most common cancer (Garniasih et al., 2020). Patients diagnosed with leukemia have a variety of treatment options, including chemotherapy, targeted and radiation therapy, or stem cell transplantation. However, while chemotherapy and radiation are intended to target cancer cells, they can also damage healthy blood cells, potentially leading to anemia.

Recent studies have suggested that herbal medicines and their phytochemical constituents, exhibiting lower or minimal toxicity, could present an appealing strategy for cancer therapy (Huang et al., 2020).

In traditional medicine, various ethnomedicinal plants are recommended for treating leukemia (Maher et al., 2021). Plant-derived bioactive compounds are valuable resources for anti-leukemic agents, given their diversity and accessibility. Mangosteen (*Garcinia mangostana* L.) is distinct due to its unique phytochemicals, xanthones (including α -mangostin, γ -mangostin, and others) (Widowati et al., 2014; Gondokesumo, 2019), which have demonstrated significant anti-cancer and anti-tumor effects (Nauman and Johnson, 2022; Novilla et al., 2016). Xan-

thones exhibit a broad spectrum of anti-cancer effects, including caspase activation, DNA cross-linking, RNA binding, inhibition of P-gp, aromatase, kinase, and topoisomerase (Kurniawan et al., 2021). α -mangostin extracted from mangosteen fruit epicarp exhibits high potential in eliminating leukemia cells (HL-60) and it possesses a high selectivity index, indicating its capability to target cancerous cells without harming healthy ones (Novilla et al., 2016).

Novel drug delivery systems (NDDS) like nanocarriers, encompassing nanoparticles and nanocrystals, are gaining prominence through their unique characteristics including high surface energy, substantial surface-to-volume ratio, and minute size compared to bulk materials (Yenurkar et al., 2023). These systems offer several advantages, including enhanced drug solubility, improved bioavailability, reduced drug dosage, and minimized side effects. Nanocrystals, specifically, stand out as carrier-free solid drug particles within the nanometer range, possessing distinct crystalline properties (Joshi et al., 2019). They play a crucial role in nanotechnology-driven approaches for tumor targeting due to their accessibility for both active and passive targeting, ensuring maximum drug content and increased bioavailability, particularly for poorly soluble drugs. The use of herbal medicines as nanocrystals has shown promise in enhancing bioavailability and solubility (Guo et al., 2023). Up to the current date, a study evaluating α -mangostin encapsulated poly (lactic-co-glycolic acid) (PLGA) nanoparticles revealed its properties in inhibiting the growth of colorectal cancer, cancer stem cells, and epithelial-mesenchymal transition (Boinpelly et al., 2020). Moreover, a prior study examined anticancer activity out of cyclodextrin-based nanoparticles with α -mangostin on CT26WT cell line. The study reported that 10 mg/kg of dosage could decline roughly 56% of the colon tumor (Meylina et al., 2021). However, research on the effects of nano-formulated medications on leukemia remains limited.

Leukemic cells often show increased activation of the Protein kinase B (AKT) signaling pathway due to genetic mutations (Wang et al., 2017). This pathway plays an important role in various cancer development aspects, including evasion of apoptosis, cell proliferation, tumor progression, and resistance to drugs. Another study showed that AKT signaling can initiate and encourage the growth of acute myeloid leukemia by regulating various downstream targets responsible for cell growth (Nepstad et al., 2020). In pediatric acute lymphoblastic leukemia, it was found that the fms Related Receptor Tyrosine Kinase 1 (FLT-1) expression could increase the survival and migration of leukemia cells (Xiu et al., 2018). Furthermore, neutralization of FLT-1 can affect leukemia localization, increase leukemia cell death, and inhibit acute lymphoblastic leukemia cell exit (Xia et al., 2022). Thus, targeting the AKT and FLT-1 genes represents an opportunity in the treatment of leukemia.

In cancer mechanisms, Reactive Oxygen Species (ROS) can contribute to the process of carcinogenesis by modifying cellular signaling pathways that regulate cell proliferation and can increase the ability of cells to avoid apoptosis (Sarmiento-

Salinas et al., 2021). Thus, ROS levels in cells must be reduced in cancer therapy. Apart from that, senescence is important in stopping the proliferation of cells that have the potential to become cancerous. This process forces cells to stop dividing and prevents tumor growth (Fakhri et al., 2022). This research was performed to analyze the effect of mangosteen peel nanocrystals (MPN) on leukemia cells (HL-60) by analyzing several parameters, namely cytotoxicity, ROS levels, senescence, and evaluating AKT and FLT-1 genes expression.

2. EXPERIMENTAL SECTION

2.1 Materials

Materials that were involved in cell line culture are Human acute promyelocytic leukemia cells (HL-60, ATCC CCL-240) that cultured in Iscove's Modified Dulbecco's Medium (IMDM, Gibco, 12440-053), 10% fetal bovine serum (FBS) (Biowest, S181B-500), 1% amphotericin B (Biowest, L0009-050), 1% antibiotic-antimycotic (Biowest, L0010-100), 1% L-Glutamine (Biowest, X0550-100), 1% minimum essential medium vitamin (Biowest, X0556-100), 1% nanomycopulitine (Biowest, L-X16-100), 0.1% gentamicin (Gibco, 15750060), and trypan blue staining (Gibco, 15250-100). Material employed in cytotoxicity assay is CCK-8 buffer (WST-8, Elabscience, E-CK-A362). Meanwhile Reactive Oxygen Species Assay comprises of ROS Fluorometric Assay Kit (Elabscience, E-BC-K138-F) and DCFH-DA reagent. Senescence assay used Senescence Cells Histochemical Staining Kit (Sigma, CS0030) and PBS 1x. Moreover, materials employed in RT-PCR method are TRI Reagent (Zymo Research, R2050-1-200), SensiFAST cDNA Synthesis Kit (Bioline, BIO-65054), and Direct-zolTM RNA Miniprep Plus (Zymo Research, R2073).

2.2 Methods

2.2.1 Preparation and Characterization of Mangosteen Peel Nanocrystals

MPN adhering to Good Manufacturing Procedure (GMP) standards (CoA No. Batch 111PV01.1) from Borobudur Natural Herbal Industry, Semarang, Indonesia, underwent 70% ethanol extraction. Nanocrystals were made in PT Nanotech Herbal Indonesia, South Tangerang, Banten. The production of nanocrystals from mangosteen peel extract is carried out using the top-down method employing the High Energy Milling Machine (HEM-Ellipse 3 Dimension), with on/off settings (2 minutes/5 minutes) for 30-60 minutes (Nugroho et al., 2019). The particle size of MPN was analyzed by Particle Size Analyzer (Beckman Coulter, Delsa Nano). The zeta potential of MPN was determined using a Zeta Potential Analyzer (HORIBA Scientific SZ-100) The morphology of MPN was investigated using scanning electron microscopy (SEM) (SEM HITACHI SU3500) (Widowati et al., 2023).

2.2.2 HL-60 Cell Line Culture

Human acute promyelocytic leukemia cells (HL-60) were acquired from Aretha Medika Utama, Biomolecular and Biomedical Research Center. The HL-60 cells were cultured in a

medium comprising Iscove's Modified Dulbecco's Medium (IMDM) that supplemented with 10% FBS, 1% antibiotic-antimycotic, 1% amphotericin B, 1% minimum essential medium vitamin, 1% L-Glutamine, 1% nanomycopulitine, 0.1% gentamicin. The HL-60 cells then incubated in an incubator (Thermo Scientific IH3543) with 5% CO₂ at 37°C. After 24 hours incubation period, the number of viable cell count was measured with a hemocytometer (Neubauer), then trypan blue staining was used to determine the number of cells sufficient for subsequent cytotoxicity assessment (Novilla et al., 2016).

2.2.3 Cytotoxicity Assay

HL-60 cells were plated in 96-well plates (Costar 3596) with a density of 1×10^4 cells per well. Cells were cultured at 37°C for 24h. The culture medium was substituted with 90 μ L new medium culture, and 10 μ L MPN (3.7, 7.8, 15.6, 31.5, 62.5, 125, 250, and 500 μ g/mL). CCK-8 buffer 10 μ L was added then incubated for 3 h. Spectrophotometer (Multiskan GO Thermo Scientific 51119300) at 450 nm wavelength was used to determine the absorbance (Chamchoy et al., 2019). The results were analyzed in terms of the viable cells percentage, the cell inhibition percentage, and the median inhibitory concentration (IC₅₀) calculation.

2.2.4 Reactive Oxygen Species Assay

ROS levels were quantified using the ROS Fluorometric Assay Kit. The experimentation involved treatments based on IC₅₀ values, specifically 0.65, 1.3, and 2.6 μ g/mL. Five distinct groups were established: (NC) negative control; (DMSO) DMSO 1%; (MPN 0.65) cells treated with 0.65 μ g/mL MPN; (MPN 1.3) cells treated with 1.3 μ g/mL MPN; and (MPN 2.6) cells treated with 2.6 μ g/mL MPN. Cells were treated overnight with MPN. After treatment, the medium was removed and DCFH-DA 10 μ M reagent 1 mL was added to the cell then incubated for 60 minutes at 37°C. The cells were harvested and washed with serum-free medium twice. A Flow Cytometer (MAQS Quant, Analyzer 10, Miltenyi Biotec (1,5,8 UV system)) was utilised for analysis (Priyandoko et al., 2022; Girsang et al., 2021).

2.2.5 Senescence Assay

Senescence cell was analyzed using the Senescence Cells Histochemical Staining Kit. Cells were plated on 6-well plates and treated with MPN (0.65, 1.3, and 2.6 μ g/mL) for 24 hours. The cell is rinsed with PBS 1 \times . Cells were fixed using fixation buffer 1 \times . for 7 minutes, then washed again. The Staining mixture was added and incubated at 37°C without CO₂ for 24 hours. Senescence cells were seen with a microscope (Olympus CKX41-F32FL) (Priyandoko et al., 2019).

2.2.6 Real-Time PCR (RT-PCR)

RNA was obtained from HL-60 cells utilizing the TRI Reagent and Direct-zolTM RNA Miniprep Plus adherence to the manual provided by the manufacturer. Total RNA yield estimation was performed using a spectrophotometer (Multiskan GO

Thermo Scientific 51119300) at 260 and 280 nm. SensiFAST cDNA Synthesis Kit was utilised to synthesize cDNA from RNA with three-stage protocol, priming, reverse transcription, and RT inactivation (Widowati et al., 2024). PCR amplification was performed using an AriaMx Real-time PCR System (Agilent, G8830A). The qPCR conditions consisted an initial pre-denaturation step for 5 minutes at 95°C, followed by qPCR 40 cycles, involving denaturation for 50 sec at 95°C, annealing for 50 sec at 58°C (GAPDH) 60°C (AKT and FLT-1), and elongation for 50 sec at 72°C. The housekeeping gene GAPDH was served as the internal control. The primers utilised for real-time PCR are outlined in Table 1. Meanwhile, Table 2 depicted the concentration and purity of RNA.

2.2.7 Statistical Analysis

The data is analyzed with SPSS (SPSS Inc; USA) using one-way ANOVA, followed by Tukey HSD post hoc test for normally distributed and homogeneous data, while Kruskal-Wallis followed by Mann Whitney test was performed for normally distributed, but not homogeneous data. *p* value ≤ 0.05 was considered as the significance value of the data. Data were visualized as mean \pm standard deviation in histograms created in the GraphPad Prism application (version 8.0.244) (Liana et al., 2019).

3. RESULTS AND DISCUSSION

3.1 Characterization of Mangosteen Peel Nanocrystal

The particle size analysis results obtained from the PSA are illustrated in Figure 1. The analysis showed that MPN exhibited a characteristic nanoparticle size with a diameter of approximately 387 nm. The zeta potential measurement results are depicted in Figure 2. The assessment of the zeta potential indicates good stability in MPN with a value of -50.5 mV. The scanning electron microscopy (SEM) results of MPN are presented in Figure 3. The SEM analysis reveals that the morphology of the nanoparticles exhibits a small spherical shape.

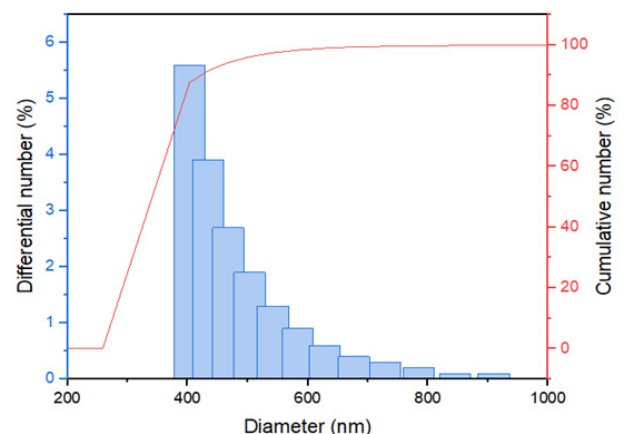


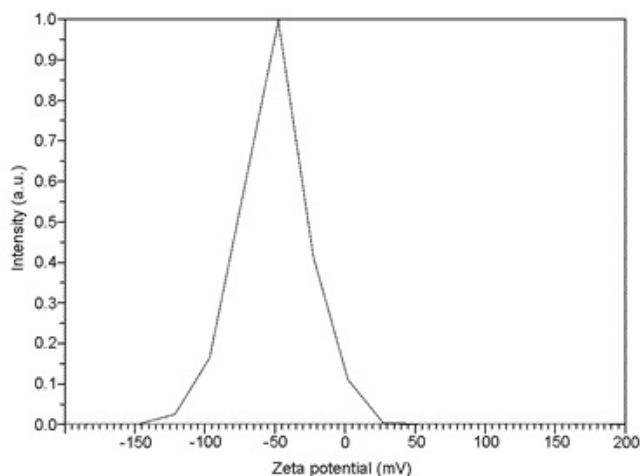
Figure 1. Particle Size Analysis Results of MPN

Table 1. Primers for Real-Time PCR

Genes	Reference	Primer Sequences (5' - 3')	Primer Length (bp)	Product Length (bp)
AKT (<i>Homo sapiens</i>)	NM_001382431.1	ACCTCAAGCTGGAGAACCT ATCTCGTACATGACCACGC	19 19	205
FLT1 (<i>Homo sapiens</i>)	NM_001160031.1	CTGGGCAGCAGACAAATCCT TGGAAGAGAAGCTTGTAGGTGG	20 22	268
GAPDH (<i>Homo sapiens</i>)	NM_001357943.2	GCCAAAAGGGTCATCATCTC TGAGTCCTTCCACGATACCA	20 20	178

Table 2. Concentration and Purity of RNA

Sample	RNA Concentration (ng/ μ L)	RNA purity (λ 260/ λ 280 nm)
Negative Control	7.200	2.185
DMSO Control	2.720	1.595
MPN 0.65 μ g/mL	7.200	2.185
MPN 1.3 μ g/mL	8.640	2.545
MPN 2.6 μ g/mL	8.720	2.547

**Figure 2.** Zeta Potential of MPN

3.2 Effect of MPN on Cytotoxicity on HL-60 Cells

The result of the cytotoxicity effect from MPN on HL-60 cells can be seen in Figure 4. At a concentration of 500 μ g/mL MPN, the viability of HL-60 cells was significantly lower than negative control (NC), indicating a decrease of -86.16% (Figure 4a). MPN demonstrated the highest inhibition percentage on HL-60 cells compared to other concentrations, displaying an inhibition rate of 186.16% (Figure 4b).

3.3 Effect of MPN on Reactive Oxygen Species Level on HL-60 Cells

The influence of MPN on ROS levels within HL-60 cells is illustrated in Figure 5. The NC exhibited the greatest ROS level (70.84%), indicating elevated ROS levels in the absence of MPN treatment. Treatment with MPN across all concentra-

tions (0.65, 1.3, and 2.6 μ g/mL) significantly reduced ROS levels compared to both NC and DMSO 1% (24.56, 27.31, and 32.24% respectively). Nevertheless, the results indicated that higher concentrations of MPN led to lowered ROS levels compared to lower MPN concentrations. This suggests the potential of MPN as a ROS scavenger.

3.4 Effect of MPN on Senescence Cells Percentage on HL-60 Cells

The evaluation of senescent cell proportions on HL-60 cells post MPN treatment was conducted utilizing Annexin V binding and PI staining, depicted in Figure 6. As per the findings, the NC exhibited the smallest percentage of senescent cells compared to all MPN treatments ($p < 0.05$). This data indicates that NC did not trigger senescence in HL-60 cells. Conversely, the administration of MPN notably escalated the count of cells undergoing senescence. Specifically, higher concentrations of MPN, particularly at 2.6 μ g/mL (67.56%), significantly led to a higher percentage of senescent cells compared to all other treatments. Overall, MPN treatment significantly increased the proportion of senescent cells in HL-60 cells, particularly at the 2.6 μ g/mL concentration.

3.5 Effect of MPN on AKT and FLT-1 Gene Expression on HL-60 Cells

The AKT gene expression in HL-60 cells after MPN administration is depicted in Figure 7a. The results demonstrate a significant decrease in AKT gene expression following MPN treatment at all concentrations compared to the NC and DMSO ($p < 0.05$). The highest concentration of MPN, 2.6 μ g/mL (0.59), induced the most substantial decrease in AKT gene expression compared to all other treatments. The analysis of FLT-1 gene expression in HL-60 cells following MPN administration is presented in Figure 7b. The resulting study indicates a significant decrease in FLT-1 gene expression after the administration of MPN at all concentrations ($p < 0.05$). Higher concentrations of MPN resulted in a more pronounced reduction in FLT-1 gene expression. *G. mangostana*, a fruit indigenous to Southeast Asia, has use for a long time in traditional Ayurvedic medicine (Kaur et al., 2020). Its pericarp is abundant in bioactive compounds like xanthenes, flavonoids, procyanidin, and benzophenones (Rizaldy et al., 2021). Our previous research shows that *G. mangostana* peel extract contains xanthenes including gartanin, γ -mangostin, α -mangostin, Smeathxanthone-A,

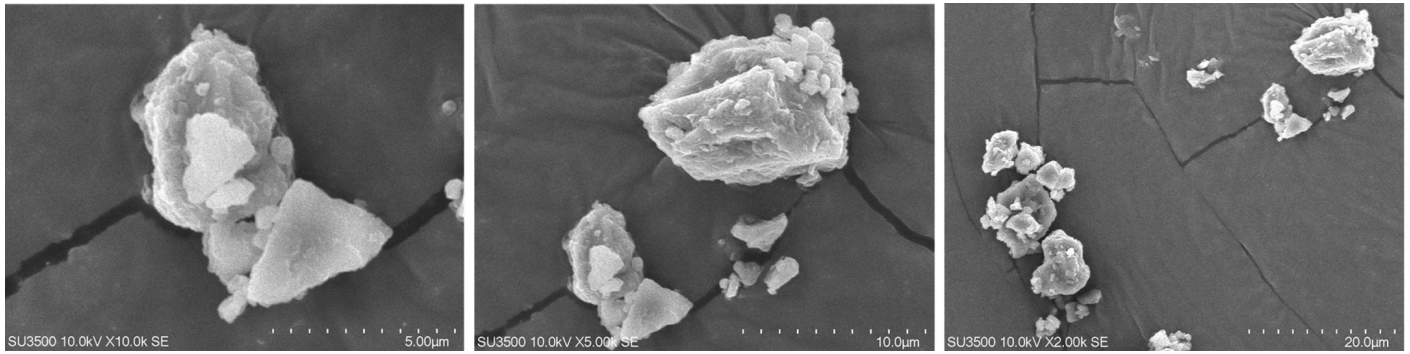


Figure 3. SEM Analysis of MPN Morphology

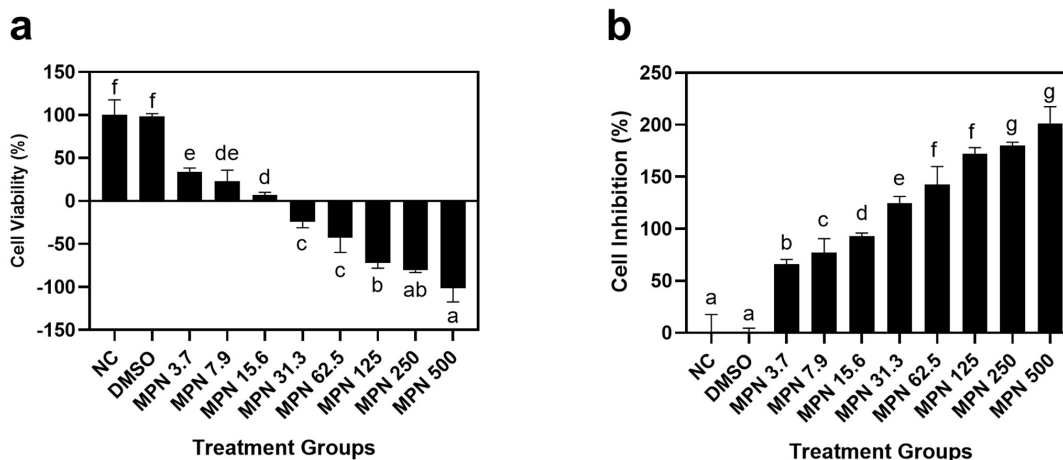


Figure 4. Effect of Various MPN Concentrations on (a) Cell Viability and (b) Cell Inhibition of HL-60 Cells.

NC: negative control; DMSO: DMSO 1%; MPN 3.7: MPN 3.7 $\mu\text{g}/\text{mL}$; MPN 7.9: MPN 7.9 $\mu\text{g}/\text{mL}$; MPN 15.6: MPN 15.6 $\mu\text{g}/\text{mL}$; MPN 31.3: MPN 31.3 $\mu\text{g}/\text{mL}$; MPN 62.5: MPN 62.5 $\mu\text{g}/\text{mL}$; MPN 125: MPN 125 $\mu\text{g}/\text{mL}$; MPN 250: MPN 250 $\mu\text{g}/\text{mL}$; MPN 500: MPN 500 $\mu\text{g}/\text{mL}$. The data is represented as mean \pm standard deviation, with distinct letters on each bar indicating significant differences among sample concentrations towards cell viability and cell inhibition based on Kruskal-Wallis followed by Mann Whitney test ($p < 0.05$).

Garcinone-C, Garcinone-D, and Garcinone E (Widowati et al., 2014; Gondokesumo, 2019). These compounds are believed to underlie the fruit's anti-inflammatory, antibacterial, and anticancer properties. Studies have shown that the pericarp of mangosteen exhibits anticarcinogenic properties, as demonstrated in various in vitro studies involving liver, breast, colorectal, lung, cervical, and prostate cancer cell lines (Verma et al., 2022). The anticancer potential of mangosteen operates through several mechanisms. It induces cell cycle arrest, inhibits cell proliferation, promotes apoptosis, and tumor cell adhesion, migration, and metastasis (Garg et al., 2023). These findings highlight the diverse ways in which mangosteen's bioactive compounds contribute to its effectiveness as a potential anticancer agent. Research by Matsumoto et al. (2003) investigated the anticancer activities of several mangosteen xanthenes on leukemia cell lines, including HL-60 and U937 cells from acute myeloid leukemia, K562 cells from chronic myeloid leukemia, and

NB4 cells from acute promyelocytic leukemia. The result showed that the xanthenes like mangostinone, garcinone E, α -mangostin, β -mangostin, γ -mangostin, and 2-isoprenyl-1,4-dihydroxy-3-methoxyxanthone which are derived from mangosteen pericarp, were discovered to hinder cell growth in all four leukemia cell lines by initiating apoptosis (Matsumoto et al., 2003; Kalick et al., 2023). α -mangostin was also found to trigger early activation of caspase-3 (Casp-3) in HL60 cells (Sheng et al., 2019).

Nanocrystals are crystalline forms of drugs that are typically ranging from 200 to 1000 nm and are stabilized or coated with a thin layer of surfactant (Arti et al., 2022). These particles have emerged as a versatile approach for delivering poorly soluble drugs. One of the key advantages of nanocrystals lies in their ability to be administered through various routes, including ophthalmic methods, enabling the creation of systems with extended retention times (McGuckin et al., 2022). Compared

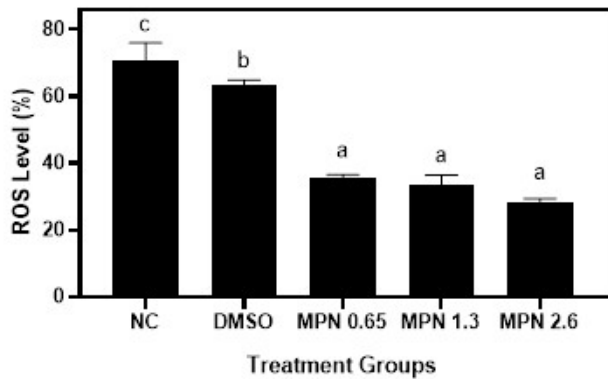


Figure 5. Effect of MPN towards ROS Level on HL-60 Cells

NC: negative control; DMSO: DMSO 1%; MPN 0.65: MPN 0.65 $\mu\text{g}/\text{mL}$; MPN 1.3: MPN 1.3 $\mu\text{g}/\text{mL}$; MPN 2.6: MPN 2.6 $\mu\text{g}/\text{mL}$. Data is presented as mean \pm standard deviation, different letters in each bar showed a significant difference among treatment towards ROS level based on Dunnett T3 post Hoc Test ($p < 0.05$).

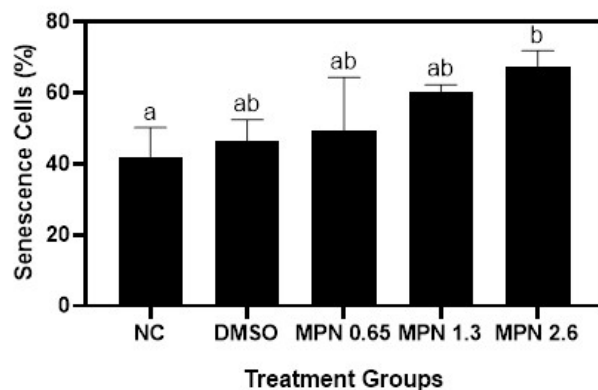


Figure 6. Effect of MPN towards Cells Senescence Percentage on HL-60 Cells

NC: negative control; DMSO: DMSO 1%; MPN 0.65: MPN 0.65 $\mu\text{g}/\text{mL}$; MPN 1.3: MPN 1.3 $\mu\text{g}/\text{mL}$; MPN 2.6: MPN 2.6 $\mu\text{g}/\text{mL}$. Data is presented as mean \pm standard deviation, different letters in each bar showed a significant difference among treatments towards cells senescence percentage based on the Tukey HSD post hoc test ($p < 0.05$).

to larger drug particles, nanocrystals exhibit superior adhesion to biological membranes. In oral delivery, this characteristic can significantly enhance drug absorption by prolonging the contact time of the drug with the surface of the gastrointestinal tract (Subramanian et al., 2022).

MPN demonstrated an average diameter of approximately 387 nm, suggesting its nanoparticle attributes are favorable for cellular absorption due to its smaller dimensions (Nagavarma

et al., 2012). Additionally, the zeta potential of MPN recorded at -50.5 mV indicated robust stability in the solution, potentially preserving the efficacy of its active constituents (Wang et al., 2022). A high zeta potential, either positive or negative, indicates the presence of a net electric charge on the nanoparticles, which can prevent particle aggregation or clumping (Grover et al., 2013). The SEM analysis uncovered nanoparticles with a small spherical shape. This nanoparticle could potentially influence the efficiency of cellular uptake (Kato et al., 2023).

Cytotoxicity assessments serve as initial screening methods in cell culture experiments, gauging how living cells respond to different substances (Aslantürk, 2018). MPN exhibited significant cellular inhibition at a concentration of 500 $\mu\text{g}/\text{mL}$ (188.24%), leading to decreased cell viability ranging from 19.72% to -86.16%. IC_{50} for MPN was 1,296 $\mu\text{g}/\text{mL}$, indicating its potency in impending cancer cell growth and survival. The level of inhibition observed in cancer cells by drugs signifies a substantial suppression of their growth, proliferation, or survival due to pharmacological interventions. This underscores the effectiveness of these drugs in halting cancer progression. Most cell lines ideally maintain a range of cell viability between 80% and 90%. Viability percentages exceeding 80% generally indicate non-cytotoxicity. Values within the 80% to 60% range are categorized as weak cytotoxicity, while those falling between 60% and 40% represent moderate cytotoxicity. Percentages below 40% indicate strong cytotoxicity (López-García et al., 2014). Other research shows that the compound α -mangostin exerts cytotoxic effects and mitochondrial dysfunction through the apoptosis induction in HL60 cells (Markowicz et al., 2019). This process was characterized by elevated levels of caspase-3 (Casp-3), Casp-9, cytochrome c release, and the release of apoptosis-inducing factors (Yu et al., 2019).

MPN exhibited a notable reduction in ROS levels within HL-60 cells at various concentrations, suggesting its potential as an effective scavenger of reactive oxygen species (ROS). However, higher concentrations of MPN resulted in decreased ROS levels compared to lower concentrations. Notably, mangosteen peel is known for its antioxidant properties, as demonstrated in various studies. Harlisa et al. (2022) found that ethyl acetate extract formulated as mangosteen peel cream reduced ROS and inhibited cell death in guinea pigs induced with UVB radiation through its antioxidant effect, regulating Tumor Necrosis Factor- α (TNF- α) and Casp-3 levels (Harlisa et al., 2022). Similarly, other research conducted on rats found that mangosteen peel infusion decreased ROS levels in rat liver and rat kidney after H_2O_2 induction (Rusman et al., 2021).

The administration of MPN resulted in a notable increase in the proportion of senescent cells within HL-60 cells, particularly at higher concentrations, implying its potential to induce cell senescence compared to the negative control. Extensive evidence from both in vitro and in vivo studies has substantiated that α -mangostin derived from mangosteen peel restrains the proliferation of various tumor cells by modulating multiple targets and signaling pathways (Herdiana et al., 2021). α -mangostin demonstrates enhanced cytotoxicity against can-

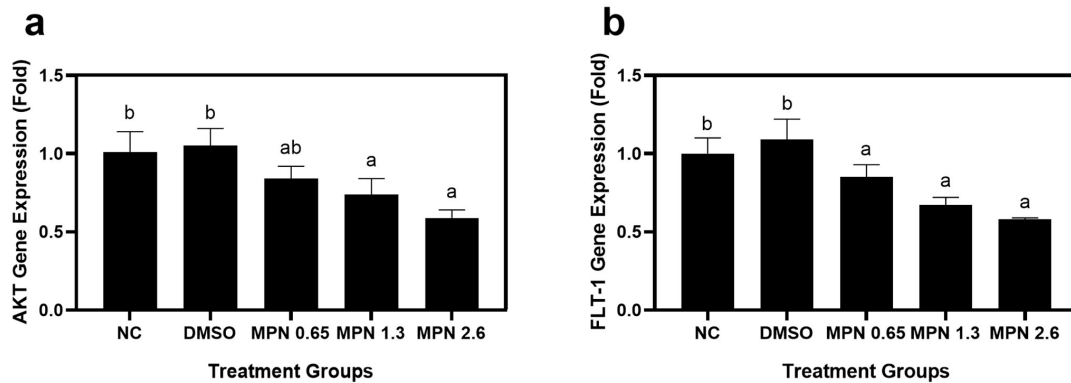


Figure 7. Effect of MPN towards (a) AKT Gene Expression (b) FLT-1 Gene Expression on HL-60 Cells

NC: negative control; DMSO: DMSO 1%; MPN 0.65: MPN 0.65 $\mu\text{g}/\text{mL}$; MPN 1.3: MPN 1.3 $\mu\text{g}/\text{mL}$; MPN 2.6: MPN 2.6 $\mu\text{g}/\text{mL}$. Data is presented as mean \pm standard deviation, different letters in each bar showed a significant difference among treatments towards AKT gene expression based on the Tukey HSD post hoc test ($p < 0.05$).

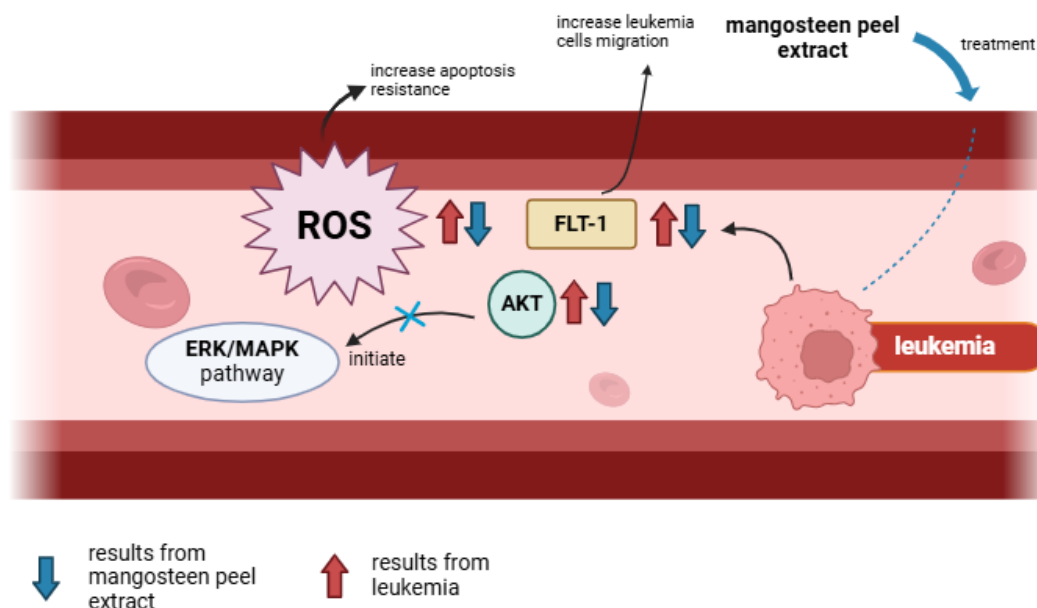


Figure 8. Proposed Mechanism of MPN on Regulating Leukemia

Leukemia condition marked by an elevated ROS and increased expression of FLT-1 and AKT. This condition intensified ERK/MAPK pathway. In addition, increased levels of ROS could increase the capacity of cells to resist apoptosis. Moreover, elevated FLT-1 in leukemia condition leads to escalated leukemia cells migration. Treatment of MPN modulated leukemia by decreasing ROS, FLT-1, and AKT expressions.

cer cells (Minute et al., 2020). Exposure to cytotoxic antitumor agents may lead to cellular aging and subsequent tumor cell demise, which can manifest through apoptosis, autophagy, or necrosis.

Following MPN treatment, there was a notable reduction in

AKT gene expression across all concentrations, with the highest concentration inducing the most significant decrease compared to other treatments. Similarly, administration of MPN led to a significant decrease in FLT-1 gene expression at all concentrations, with higher MPN concentrations resulting in a more

pronounced reduction. Studies conducted by Ma et al. (2017) demonstrated that diminished AKT gene expression inhibits the ERK/MAPK pathway, resulting in inhibit leukemia cell proliferation. Additionally, Amini et al. (2013) investigated the role of soluble FLT-1 (sFLT-1) in acute myeloid leukemia (AML), suggesting that targeting FLT-1 could be a promising strategy for AML treatment by employing nonviral gene carriers to deliver sFLT-1 for effective antiangiogenic gene therapy (Amini et al., 2013). Figure 8 depicts the proposed mechanism of MPN on regulating leukemia by modulating ROS, AKT, and FLT-1. This highlights the potential involvement of FLT-1 in AML progression and the potential for targeted interventions in its treatment.

4. CONCLUSIONS

MPN exhibited characteristics such as a diameter in the nanometer range and displaying good stability. MPN significantly reduced cell viability and notably inhibited cell growth at a specific concentration. MPN treatment led to a reduction in ROS levels in HL-60 cells. Notably, MPN treatment induced an escalation in senescent cell proportions, particularly at higher concentrations, indicating a potential induction of cell senescence. Additionally, MPN treatment resulted in significant decreases in AKT and FLT-1 gene expressions at all concentrations. Overall, these findings highlight the diverse impacts of MPN on HL-60 leukemia cells, suggesting potential implications for its cytotoxic, senescence-inducing, and gene expression-modulating properties in leukemia cell models.

5. ACKNOWLEDGMENT

The authors gratefully appreciated the Competitive National Research-Fundamental Research 2023, Minister of Education, Culture, Research, and Technology of the Republic of Indonesia for funding support with grant number of 183/E5/PG.02.00.PL/2023. Moreover, we thank Adilah Hafizha Nur Sabrina, Annisa Firdaus Sutendi, Faradhina Salfa Nindya, and Vini Ayuni for their helpful assistance and PT Industri Jamu Borobudur Semarang-Indonesia for preparing the mangosteen peel extract with GMP standard.

REFERENCES

- Amini, R., A. Jalilian, A. Veerakumarasivam, S. Abdullah, A. Abdulamir, and F. Nadali (2013). Soluble Flt-1 Gene Delivery in Acute Myeloid Leukemic Cells Mediating a Non-viral Gene Carrier. *BioMed Research International*, **2013**; 1–8
- Arti, S., M. Bharti, V. Kumar, V. Rehani, and J. Dhiman (2022). Drug Nanocrystals as Nanocarrier-Based Drug Delivery Systems. *Industrial Applications of Nanocrystals*, **16**; 179–203
- Aslantürk, O. (2018). In Vitro Cytotoxicity and Cell Viability Assays: Principles, Advantages, and Disadvantages. *Genotoxicity—A Predictable Risk to Our Actual World*, **2**; 64–80
- Boinpelly, V., R. Verma, S. Srivastav, R. Srivastava, and S. Shankar (2020). α -Mangostin-Encapsulated PLGA Nanoparticles Inhibit Colorectal Cancer Growth by Inhibiting Notch Pathway. *Journal of Cellular and Molecular Medicine*, **24**; 11343–11354
- Chamchoy, K., D. Pakotiprapha, P. Pumirat, U. Leartsakulpanich, and U. Boonyuen (2019). Application of WST-8 Based Colorimetric NAD(P)H Detection for Quantitative Dehydrogenase Assays. *BMC Biochemistry*, **20**; 1–14
- Dong, Y., O. Shi, Q. Zeng, X. Lu, W. Wang, and Y. Li (2020). Leukemia Incidence Trends at the Global, Regional, and National Level Between 1990 and 2017. *Experimental Hematology & Oncology*, **9**; 1–11
- Fakhri, S., S. Moradi, L. DeLiberto, and A. Bishayee (2022). Cellular Senescence Signaling in Cancer: A Novel Therapeutic Target to Combat Human Malignancies. *Biochemical Pharmacology*, **199**; 114989
- Garg, P., R. Garg, D. Horne, S. Awasthi, R. Salgia, and S. Singhal (2023). Prognostic Significance of Natural Products Against Multidrug Tumor Resistance. *Cancer Letters*, **557**; 216079
- Garniasih, D., S. Susanah, Y. Sribudiani, and D. Hilmanto (2020). The Incidence and Mortality of Childhood Acute Lymphoblastic Leukemia in Indonesia: A Systematic Review and Meta-Analysis. *PLoS ONE*, **17**; e0269706
- Girsang, E., C. N. Ginting, I. N. Lister, K. Y. Gunawan, and W. Widowati (2021). Anti-Inflammatory and Antiaging Properties of Chlorogenic Acid on UV-Induced Fibroblast Cell. *PeerJ*, **9**; e11419
- Gondokesumo, M. E. (2019). Xanthenes Analysis and Antioxidant Activity Analysis (Applying ESR) of Six Different Maturity Levels of Mangosteen Rind Extract (*Garcinia mangostana* Linn.). *Pharmacognosy Journal*, **11**; 369–373
- Grover, I. S., S. Singh, and B. Pal (2013). The Preparation, Surface Structure, Zeta Potential, Surface Charge Density and Photocatalytic Activity of TiO₂ Nanostructures of Different Shapes. *Applied Surface Science*, **280**; 366–372
- Guo, M., S. Qin, S. Wang, M. Sun, H. Yang, and X. Wang (2023). Herbal Medicine Nanocrystals: A Potential Novel Therapeutic Strategy. *Molecules*, **28**; 6370
- Harlisa, P., H. K. Sentono, B. Purwanto, and P. Dirgahayu (2022). The Ethyl Acetate Extract of Mangosteen Peel Cream Attenuates Ultraviolet B Radiation-Induced Apoptotic Cell Death Via Antioxidant Effect by Regulation TNF- α and Caspase 3 in Guinea Pig Skin. *Bangladesh Journal of Medical Science*, **21**; 512–520
- Herdiana, Y., N. Wathoni, S. Shamsuddin, and M. Muchtaridi (2021). α -Mangostin Nanoparticles Cytotoxicity and Cell Death Modalities in Breast Cancer Cell Lines. *Molecules*, **26**; 5119
- Huang, M., J. J. Lu, and J. Ding (2020). Natural Products in Cancer Therapy: Past, Present and Future. *Natural Products and Bioprospecting*, **11**; 5–13
- Joshi, K., A. Chandra, K. Jain, and S. Talegaonkar (2019). Nanocrystalization: An Emerging Technology to Enhance the Bioavailability of Poorly Soluble Drugs. *Pharmaceutical Nanotechnology*, **7**; 259–278

- Kalick, L. S., H. A. Khan, E. Maung, Y. Baez, A. N. Atkinson, and C. E. Wallace (2023). Mangosteen for Malignancy Prevention and Intervention: Current Evidence, Molecular Mechanisms, and Future Perspectives. *Pharmaceutical Research*, **188**; 106630
- Kato, C., M. Itaya-Takahashi, T. Miyazawa, J. Ito, I. S. Parida, and H. Yamada (2023). Effects of Particle Size of Curcumin Solid Dispersions on Bioavailability and Anti-Inflammatory Activities. *Antioxidants*, **12**; 724
- Kaur, G., A. Singh, and B. N. Dar (2020). Mangosteen (*Garcinia mangostana* L.). In G. A. Nayik and A. Gull, editors, *Antioxidants in Fruits: Properties and Health Benefits*. Springer, Singapore
- Kurniawan, Y., K. Priyanga, Jumina, H. Pranowo, E. Sholikhah, and A. Zulkarnain (2021). An Update on the Anticancer Activity of Xanthone Derivatives: A Review. *Pharmaceuticals*, **1**; 1144
- Liana, L., R. Rizal, W. Widowati, F. Fioni, K. Akbar, E. Fachrial, and I. Lister (2019). Antioxidant and Anti-Hyaluronidase Activities of Dragon Fruit Peel Extract and Kaempferol-3-O-Rutinoside. *Jurnal Kedokteran Brawijaya*, **30**; 247–252
- López-García, J., M. Lehocný, P. Humpolíček, and P. Sáha (2014). HaCaT Keratinocytes Response on Antimicrobial Atelocollagen Substrates: Extent of Cytotoxicity, Cell Viability and Proliferation. *Journal of Functional Biomaterials*, **5**; 43–57
- Ma, L., Z. Xu, J. Wang, Z. Zhu, G. Lin, and L. Jiang (2017). Matrine Inhibits BCR/ABL Mediated ERK/MAPK Pathway in Human Leukemia Cells. *Oncotarget*, **8**; 108880
- Maher, T., R. Raus, D. Daddiouaissa, F. Ahmad, N. Adzhar, E. Latif, F. Abdulhafiz, and A. Mohammed (2021). Medicinal Plants with Anti-Leukemic Effects: A Review. *Molecules*, **26**; 2741
- Markowicz, J., Ł. Uram, J. Sobich, L. Mangiardi, P. Maj, and W. Rode (2019). Antitumor and Anti-Nematode Activities of 03B1-Mangostin. *European Journal of Pharmacology*, **863**; 172678
- Matsumoto, K., Y. Akao, E. Kobayashi, K. Ohguchi, T. Ito, and T. Tanaka (2003). Induction of Apoptosis by Xanthones from Mangosteen in Human Leukemia Cell Lines. *Journal of Natural Products*, **66**; 1124–1127
- McGuckin, M., J. Wang, R. Ghanma, N. Qin, S. Palma, and R. Donnelly (2022). Nanocrystals As a Master Key To Deliver Hydrophobic Drugs Via Multiple Administration Routes. *Journal of Controlled Release*, **345**; 334–353
- Meylina, L., M. Muchtaridi, I. Joni, A. Mohammed, and N. Wathoni (2021). Nanoformulations of 03B1-Mangostin for Cancer Drug Delivery System. *Pharmaceutics*, **13**; 1–21
- Minute, L., A. Teijeira, A. Sanchez-Paulete, M. Ochoa, M. Alvarez, and I. Otano (2020). Cellular Cytotoxicity Is a Form of Immunogenic Cell Death. *Journal of Immunotherapy for Cancer*, **8**; 1–14
- Nagavarma, B., H. Yadav, A. Ayaz, L. Vasudha, and H. Shivakumar (2012). Different Techniques for Preparation of Polymeric Nanoparticles-A Review. *Asian Journal of Pharmaceutical and Clinical Research*, **5**; 16–23
- Nauman, M. and J. Johnson (2022). The Purple Mangosteen (*Garcinia mangostana*): Defining the Anticancer Potential of Selected Xanthones. *Pharmaceutical Research*, **175**; 106032
- Nepstad, I., K. J. Hatfield, I. S. Grønningseter, and H. Reikvam (2020). The PI3K-Akt-mTOR Signaling Pathway in Human Acute Myeloid Leukemia (AML) Cells. *International Journal of Molecular Sciences*, **21**; 2907
- Novilla, A., D. S. Djamhuri, N. Fauziah, M. Maesaroh, B. Balqis, and W. Widowati (2016). Cytotoxic Activity of Mangosteen (*Garcinia mangostana* L.) Peel Extract and α -Mangostin Toward Leukemia Cell Lines (HL-60 and K-562). *Journal of Natural Remedies*, **16**; 52–59
- Nugroho, D., D. Daratika, E. Agustin, M. Kamila, M. Rifada, and L. Togatorop (2019). Characteristic of *Garcinia mangostana*'s Pericarp Prepared by Mechanical Milling. In *Proceedings of the 16th ASEAN Food Conference*. Bali, Indonesia, pages 15–18
- Priyandoko, D., W. Widowati, and K. Y. Gunawan (2019). Ethanolic Extract of Moringa's Leaves (*Moringa oleifera*) Induce Senescence on Adenocarcinomic Alveolar Basal Epithelial Cells (A549 Cell-Lines). *Proceeding of International Conference on Science, Health, and Technology*; 156–159
- Priyandoko, D., W. Widowati, W. Widodo, K. Kusdianti, H. Hernawati, and W. S. Widodo (2022). The Potential of *Moringa oleifera* Leaf Ethanolic Extract as Anticancer Against Lung Adenocarcinoma (A549) Cells and Its Toxicity on Normal Mammary Cells (MCF-12A). *Trends in Sciences*, **19**; 3202
- Rizaldy, D., R. Hartati, T. Nadhifa, and I. Fidrianny (2021). Chemical Compounds and Pharmacological Activities of Mangosteen (*Garcinia mangostana* L.)-Updated Review. *Biointerface Research in Applied Chemistry*, **12**; 2503–2516
- Rusman, J. R., S. A. Sundari, A. Nuriliani, and H. T. Saragih (2021). Ameliorative Effect of Mangosteen (*Garcinia mangostana* L.) Peel Infusion on the Histopathological Structures of the Liver and Kidney of Rats (*Rattus norvegicus* Berkenhout, 1769) After H₂O₂ Induction. *Veterinary World*, **14**; 1579
- Sarmiento-Salinas, F. L., A. Perez-Gonzalez, A. Acosta-Casique, A. Ix-Ballote, A. Diaz, and S. Trevino (2021). Reactive Oxygen Species: Role in Carcinogenesis, Cancer Cell Signaling and Tumor Progression. *Life Sciences*, **284**; 119942
- Sheng, X., J. Li, C. Zhang, L. Zhao, L. Guo, and T. Xu (2019). α -Mangostin Promotes Apoptosis of Human Rheumatoid Arthritis Fibroblast-Like Synoviocytes by Reactive Oxygen Species-Dependent Activation of ERK1/2 Mitogen-Activated Protein Kinase. *Journal of Cellular Biochemistry*, **120**; 14986–14994
- Subramanian, D. A., R. Langer, and G. Traverso (2022). Mucus Interaction to Improve Gastrointestinal Retention and Pharmacokinetics of Orally Administered Nano-Drug Delivery Systems. *Journal of Nanobiotechnology*, **20**; 1–23

- Verma, N., S. Pandit, A. Kumar, G. Yadav, S. K. Giri, and D. Lahiri (2022). Recent Update on Active Biological Molecules in Generating the Anticancerous Therapeutic Potential of *Garcinia Mangostana*. *Applied Biochemistry and Biotechnology*, **194**; 4724–4744
- Wang, W., B. Zhang, Y. Shi, D. Zhou, and R. Wang (2022). Improvement in Dispersion Stability of Alumina Suspensions and Corresponding Chemical Mechanical Polishing Performance. *Applied Surface Science*, **597**; 153703
- Wang, Y., H. Mo, J. Gu, K. Chen, Z. Han, and Y. Liu (2017). Cordycepin Induces Apoptosis of Human Acute Monocytic Leukemia Cells via Downregulation of the ERK/Akt Signaling Pathway. *Experimental and Therapeutic Medicine*, **14**; 3067–3073
- Widowati, W., L. Darsono, J. Suherman, Y. Yellianty, and M. Maesaroh (2014). High Performance Liquid Chromatography (HPLC) Analysis, Antioxidant, Antiaggregation of Mangosteen Peel Extract (*Garcinia mangostana* L.). *International Journal of Bioscience, Biochemistry, and Bioinformatics*, **4**; 458
- Widowati, W., D. Priyandoko, L. Lenny, R. Revika, S. Novianti, and H. S. W. e. a. Kusuma (2024). *Camellia sinensis* L. Extract Suppresses Inflammation on Acute Respiratory Distress Syndrome Cells Models via Decreasing IL-1 β , IL-6 and COX-2 Expressions. *Trends in Sciences*, **21**; 7010
- Widowati, W., T. L. Wargasetia, V. Kurniawati, R. Rachmaniar, V. A. Yuninda, and A. H. Sabrina (2023). In-Vitro Study of Potential Antioxidant Activities of Mangosteen and Its Nanoemulsions. *Medicinal Plants-International Journal of Phytomedicine*, **15**; 534–542
- Xia, J., M. Wang, Y. Zhu, C. Bu, and T. Li (2022). Differential mRNA and Long Noncoding RNA Expression Profiles in Pediatric B-Cell Acute Lymphoblastic Leukemia Patients. *BMC Pediatrics*, **22**; 1–11
- Xiu, B., W. Zhang, B. Huang, J. Chen, H. Lu, and J. Fu (2018). Genetic Inhibition of Vascular Endothelial Growth Factor Receptor-1 Significantly Inhibits the Migration and Proliferation of Leukemia Cells and Increases Their Sensitivity to Chemotherapy. *Oncology Reports*, **29**; 2030–2038
- Yenurkar, D., M. Nayak, and S. Mukherjee (2023). Recent Advances of Nanocrystals in Cancer Theranostics. *Nanoscale Advances*, **5**; 4018–4040
- Yu, T., X. Huang, J. Liu, Q. Fu, B. Wang, and Z. Qian (2019). Polymeric Nanoparticles Encapsulating *alpha*-Mangostin Inhibit the Growth and Metastasis in Colorectal Cancer. *Applied Materials Today*, **16**; 351–366